

Quasicontinuum Monte Carlo Simulation of Multilayer Surface Growth

Jason P. DeVita, Leonard M. Sander, and Peter Smereka

Abstract. We develop a method, for simulating epitaxial growth, based on coarse graining (in time) the evolution equations of the probability functions for Kinetic Monte Carlo. Our approach has the advantages offered by continuum methods but still retains enough of the fluctuations to offer good physical fidelity. We have compared our method to KMC in a number of situations and found good agreement.

Keywords. Epitaxial Growth, Kinetic Monte Carlo, Quasicontinuum.

1. Introduction

Molecular beam epitaxy (MBE) is a popular technique for growing materials, and is also an interesting example of a statistical process out of equilibrium. Epitaxy is commonly modeled by either kinetic monte-carlo (KMC) or by continuum methods. In KMC, discrete adatoms are deposited onto a grid (taken to be a square lattice for simplicity) at a rate F . Once on the grid, they execute nearest neighbor hops with probability $e^{(-nE_0/kT)}$, where E_0 is the bond energy between two adatoms, and n is the number of in-plane bonds. KMC automatically incorporates internal noise by representing each atom individually. However, in situations where the adatom density is high – such as near equilibrium – KMC can be slowed down considerably.

Continuum models such as those proposed by Burton et al.[1] and Ghez & Lyer[2] do not slow down for large adatom densities. In this approach, adatoms are represented as a continuous field. This type of model has been implemented using level set methods, see for example Refs [3, 4, 5]. These models have the potential to be much faster than KMC when there are a large number of adatoms present occurs in the presence of high detachment rates [6]. In addition, there are situations where it is believed that that epitaxial growth occurs quite close to equilibrium. In these situations there is a large number of adatoms present and such systems

become very difficult to simulate using KMC. One such example is Tersoff et al. [7].

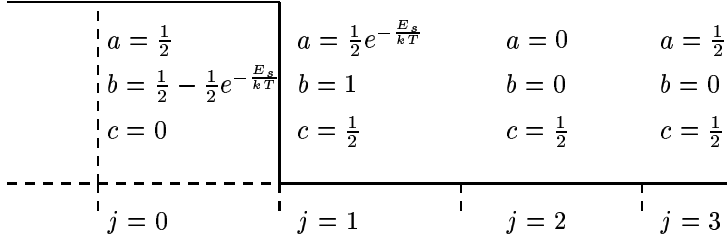
There have been other approaches that are continuum in nature but capture certain aspects of the discrete nature of the problem. E and Schulze[8] developed a formulation, in one space dimension, with discrete adatoms; the adatoms were attached deterministically to islands. Mandreoli et al. [9] presented a similar idea in two dimensions. Both of these formulations will be discussed in more detail later in the paper. We also mention that Ratsch et al.[10] were able to include finite size effects in a continuum model.

In all of the continuum formulations outlined above fluctuations which may be important are ignored. One important kind of fluctuation arises from that fact that particles are attached to the interface stochastically one at a time. This effect is responsible for the fractal-like patterns that are observed in diffusion-limited growth; see Witten and Sander[11]. In an effort to retain the advantages of the continuum approach and include fluctuations Schulze et al.[12] developed a hybrid approach in one space dimension. In this formulation the regions near the interface are treated with KMC. Non-KMC regions are course-grained in space and time and treated in the continuum field. This approach is best suited for situations with widely spaced steps and has been extended to two space dimensions by Schulze[13].

Another hybrid approach was proposed in Ref.[14]. In this work the authors considered a situation where the interface was commensurate with the underlying lattice. They then solve the diffusion equation with boundary conditions on the interface that include effects of detachment and attachment. Adatoms are added or removed as follows. The net flux of adatoms to the interface and from the interface are computed. When either of these exceeds unity adatoms are added or removed with a probability proportional to this flux. In this way effects of fluctuations are included. This approach is reminiscent of the dielectric breakdown model [16]. The advantage of this approach is that it allows large time steps because the boundary conditions naturally include the effects of rapid attachment and detachment. In addition, the speed of the algorithm is independent of the number of adatoms since adatoms are treated in terms of a probability density. The disadvantage is that the computation is at every site. To go significantly faster it is necessary to take very large time steps which entails coarse graining in time.

2. Probabilistic KMC and Coarse-Graining

In this section we will combine ideas from KMC, E and Schulze, Mandreoli et al. [9] and Russo et al. [14] to formulate our temporally coarse grained model for epitaxial growth. To fix ideas we first work in one dimension and consider very simple model. At each time step an adatom must hop. It will hop to the left or right with equal probability. We will consider the situation where the sites left of $j = 0$ are occupied by island atoms and there is no detachment. Note that $j = 1$ is a potential attachment site. Let p_j^n represent the adatom concentration at site


 FIGURE 1. How the geometry determines a , b , and c .

j at time n . The time evolution of p_j^n is then given by

$$p_j^{n+1} = \frac{1}{2}(p_{j+1}^n + p_{j-1}^n) + F \quad \text{for } j = \dots, -3, -2, -1 \quad (2.1)$$

$$p_0^{n+1} = \frac{1}{2}p_{-1}^n + F \quad (2.2)$$

$$p_1^{n+1} = p_1^n + \frac{1}{2}(p_2^n + p_0^n) + F \quad (2.3)$$

$$p_2^{n+1} = \frac{1}{2}p_3^n + F \quad (2.4)$$

$$p_j^{n+1} = \frac{1}{2}(p_{j+1}^n + p_{j-1}^n) + F \quad \text{for } j = 3, 4, 5, \dots \quad (2.5)$$

Eqs. (2.1) and (2.5) describe the adatom hopping on top of the island and below the island respectively and away from the step. This can be understood from the fact that adatoms can hop into these sites from either the left or right. Since the attachment is irreversible, Eqs (2.2) and (2.4) will not have any contribution from the attachment site ($j = 1$). Finally since $j = 1$ is an attachment site any adatoms that arrive there cannot leave. This is reflected in the first term in Eq. (2.3). Therefore, p_1^n represents the net mass of adatoms at the attachment site.

The expression for p_j^n can be written as

$$p_j^{n+1} = a_j p_{j+1}^n + b_j p_j^n + c_j p_{j-1}^n + F$$

where a_j , b_j , and c_j are determined by the environment, as shown in figure 2. A flux of adatoms has now been included with the F term. We can modify this formulation to include an Ehrlich-Schwoebel Barrier [15]. In this case, a_j , b_j and c_j are determined as shown in figure 2. We can rewrite the evolution equation as

$$p_j^{n+1} - p_j^n = a_j p_{j+1}^n + (b_j - 1)p_j^n + c_j p_{j-1}^n + F \quad (2.6)$$

We make the assumption that p is slowly varying in time and use the following approximation:

$$\frac{d}{dt} p_j \approx p_j^{n+1} - p_j^n$$

3	$a^x = 1/4$ $c^x = 1/4$ $a^y = \frac{1}{4}e^{-E_s/kT}$ $c^y = 1/4$ $b = 1$	$a^x = 0$ $c^x = 1/4$ $a^y = 0$ $c^y = 1/4$ $b = 0$	$a^x = 1/4$ $c^x = 1/4$ $a^y = 1/4$ $c^y = 1/4$ $b = 0$	$a^x = 1/4$ $c^x = 1/4$ $a^y = 1/4$ $c^y = 1/4$ $b = 0$
2	$a^x = 0$ $c^x = 0$ $a^y = 1/4$ $c^y = 0$ $b = \frac{3}{4}(1 - e^{-E_s/kT})$	$a^x = \frac{1}{4}e^{-E_s/kT}$ $c^x = 1/4$ $a^y = \frac{1}{4}e^{-E_s/kT}$ $c^y = 1/4$ $b = 1$	$a^x = 0$ $c^x = 1/4$ $a^y = 0$ $c^y = 1/4$ $b = 0$	$a^x = 1/4$ $c^x = 1/4$ $a^y = 1/4$ $c^y = 1/4$ $b = 0$
1	$a^x = 0$ $c^x = 1/4$ $a^y = 0$ $c^y = 1/4$ $b = \frac{1}{2}(1 - e^{-E_s/kT})$	$a^x = 1/4$ $c^x = 0$ $a^y = 0$ $c^y = 0$ $b = \frac{3}{4}(1 - e^{-E_s/kT})$	$a^x = \frac{1}{4}e^{-E_s/kT}$ $c^x = 1/4$ $a^y = 1/4$ $c^y = 1/4$ $b = 1$	$a^x = 0$ $c^x = 1/4$ $a^y = 1/4$ $c^y = 1/4$ $b = 0$
	1	2	3	4

FIGURE 2. Computation of a, b and c in two dimensions

and write (2.6) as

$$\frac{d}{dt}p_j(t) = a_j p_{j+1}(t) + (b_j - 1)p_j(t) + c_j p_{j-1}(t) + F$$

We can easily extend this to two space dimensions, as follows:

$$\frac{d}{dt}p_{i,j} = \Delta p_{i,j} + F \quad (2.7)$$

where

$$\Delta p_{i,j} \equiv a_{ij}^x p_{i-1,j} + c_{ij}^x p_{i+1,j} + a_{ij}^y p_{i,j-1} + c_{ij}^y p_{i,j+1} + (b_{i,j} - 1)p_{i,j} + F$$

where a, b and c are determined by the environment as shown in Figure 2.

A formulation similar to this was developed in one dimension by E and Schulze[8] and by Mandreoli et al.[9]. In both these approaches an adatom is added to an island edge when the attachment probability exceeds one. Therefore these models are deterministic and consequently ignore fluctuations. Indeed, in Ref.[9] the authors report not being able to obtain fractal island shapes.

In our approach we attach adatoms probabilistically. Let A represent all potential attachment sites. Then

$$P = \sum_{(i,j) \in A} p_{i,j}^n$$

represents the total mass of adatoms in the attachment sites. When the integer part of P exceeds unity then then we add L adatoms to attachment sites where

$L = [P]$ (L is the integer part of P) The attachment location is chosen at random with a probability proportional to p_i^n .

2.1. Edge Diffusion and Detachment

The effects of edge diffusion and detachment are incorporated by using KMC on the edge atoms (atoms with less than 4 in-plane bonds). The difficulty with this procedure is that these atoms may hop off the island at which point they should become part of the adatom sea. To incorporate these adatoms we place a source term concentrated at the point of detachment with a strength equal to $1/\Delta t$ where Δt is the time step.

2.2. Nucleation

For nucleation we use a variant of the nucleation model introduced in [4, 5]. In this model adatoms are removed at a rate $2\sigma_1 \sum_{i,j} (p_{i,j}^n)^2$ from the adatom field. σ_1 is the capture rate and its computation is discussed in Refs. [17, 3, 19]. Using the approach taken in [19], the capture number typically takes on values of 3 ± 1 for situations we're simulating. Empirical results from our simulations show little dependence on σ_1 over such a variation; thus, in our computations we take $\sigma_1 = 3$. When this exceeds unity, dimer(s) are added to the surface. The location of the dimer is chosen at random with a probability proportional to $p^2(x, t)$. Due to detachment, the adatom concentration is will be high near the interface. To reduce the effects of an adatom nucleating with itself we only allow nucleation in a region at least two grid cells from the interface. We call this region Ω .

3. The Algorithm

Step 1. Compute $\Delta p_{i,j}$ as described in Figure 2 and solve the diffusion equation implicitly for one time step from t_n to $t_{n+1} = t_n + \Delta t$.

$$\dot{p}_{i,j} = \Delta p_{i,j} + F - 2\sigma_1 \sum_{(i,j) \in \Omega} (p_{i,j}^n)^2 + \frac{1}{\Delta t} \sum_{(i,j) \in D} \delta_{i,j} \quad (3.1)$$

the updated value of p is denoted p^{n+1} and Ω is defined in §2.2. The diffusion equation is solved implicitly using operator splitting. D is the set of detachment sites and is computed in Step 3.

Step 2. Identify all the attachment sites and then compute

$$P = P^* + \sum_{(i,j) \in A} p_{i,j}^{n+1}$$

where P^* is defined below. If $P > 1$ then $L = [P]$ adatoms are attached. The location is chosen at random with a probability distribution based on the values of p at the attachment sites. This performed using rejection Monte Carlo. Then set $P^* = P - L$ and $p_{i,j} = 0$ for $(i, j) \in A$.

Step 3. Now we execute KMC on the edge atoms. Suppose there are M edge atoms. Then we choose $M\Delta t$ edge atoms at random, and allow each to hop with

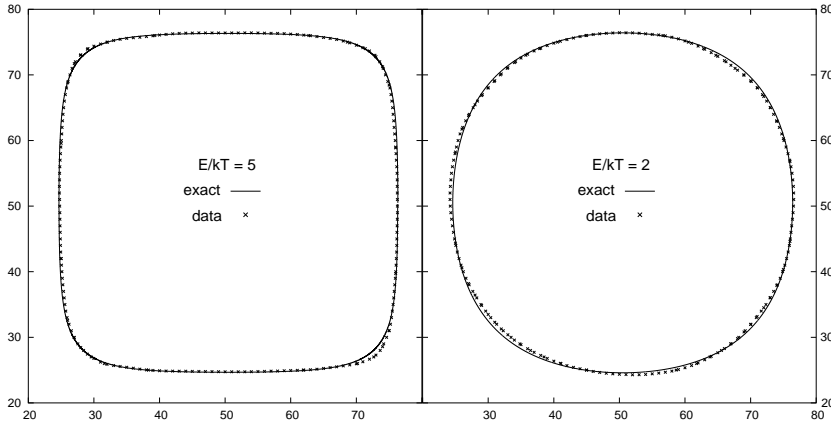


FIGURE 3. Our method produces equilibrium island shapes that closely match the exact shapes [18]. The plots are for E/kT of 5 (left) and 2 (right).

probability $\exp(-nE_0/kT)$, where E_0 is the bond energy, and n is the number of in-plane nearest-neighbor bonds. If an atom hops to a site which is not adjacent to an edge we say it has detached. Denote the set of detachment sites by D . The set D is used in Step 1.

Step 4. Finally, we nucleate new islands, by introducing new dimers. The rate of dimer nucleation is given by the sum of $\sigma_1 p^2$ over all sites that are at least two grid point from an interface. The prefactor σ_1 represents the cross-section for adatom capture by another adatom.

4. Results

Our method produces accurate results for both submonolayer and multilayer growth.

4.1. Submonolayer growth

With the flux F set to 0 and the initial condition of a square island, we allowed the island to come to equilibrium with the surrounding adatoms. Figure 3 shows a comparison of QCMC generated equilibrium island shapes compared to exact solutions for two different temperatures. The exact solutions are according to [18]. The data is averaged over 80 and 200 realizations, for $E/kT = 5$ and $E/kT = 2$ respectively.

Figure 4 shows early growth (0.1ML) for two different growth regimes. One is grown at $E/kT = 3.5$ and produces compact islands. The other is at zero temperature, which produces dendritic islands. In both cases, QCMC compares qualitatively with KMC.

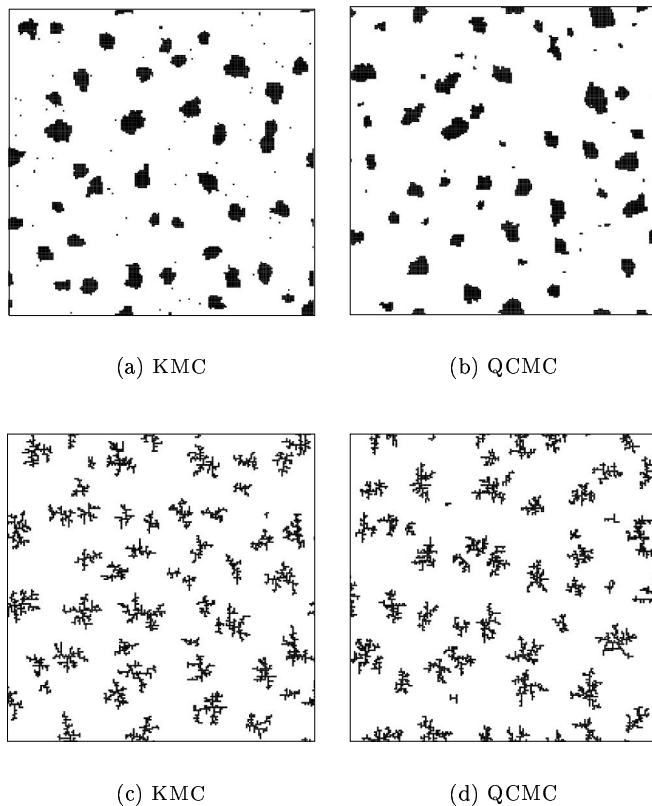


FIGURE 4. Submonolayer growth, comparing KMC to QCMC, for two different growth regimes. Figures (a) and (b) were grown at $D/F = 2.5 \times 10^5$, $E/kT = 3.5$, for 0.1ML. Figures (c) and (d) were grown at $D/F = 5 \times 10^6$, $T = 0$, for 0.1ML. QCMC and KMC produce qualitatively similar results for growth of both compact and dendritic islands.

4.2. Multilayer growth and mounding

An interesting case of multilayer growth is development in the presence of an Ehrlich-Schwoebel (ES) barrier, which can produce mounding [20, 21]. The fundamental process is that the barrier traps adatoms on the top of islands, and leads to nucleation there, so that the growth cannot be layer-by-layer. Figure 5 shows KMC and QCMC results for multilayer growth with no ES barrier. Figure 6 shows a comparison of KMC and QCMC for multilayer growth involving barrier-induced mounding. We qualitatively reproduce the KMC patterns.

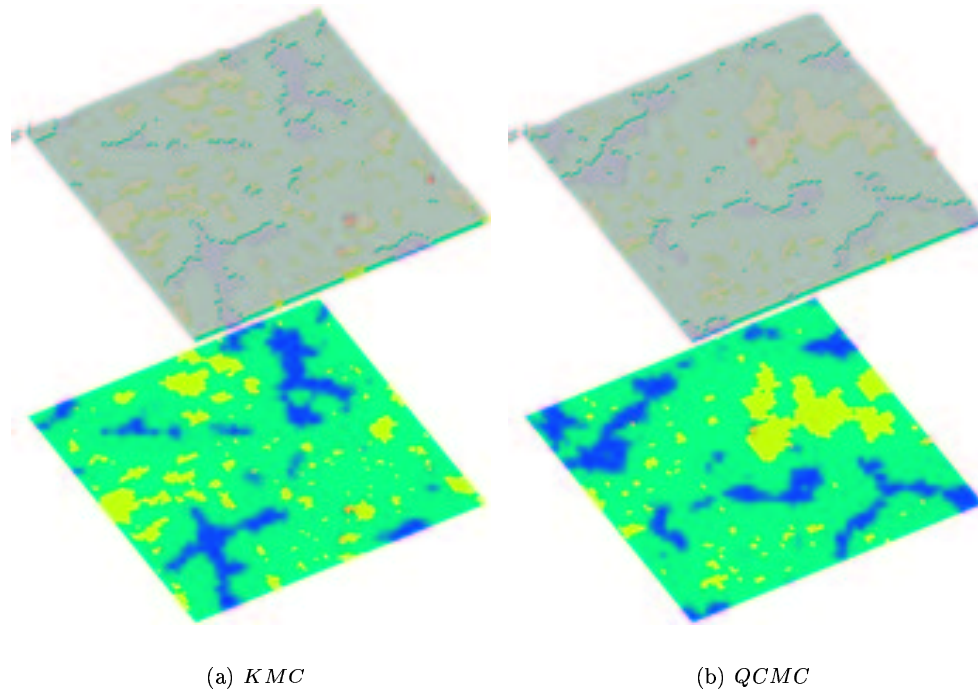


FIGURE 5. KMC versus QCMC for no ES barrier, $E_0/kT = 3.5$, $F = 0.5 \times 10^{-4}$, 50 monolayers

References

- [1] W.K. Burton, N. Cabrera, and F.C. Frank, *The growth of crystals and the equilibrium structure of their surfaces*, Trans. R. Soc. London Ser. A **243**, 299 (1951).
- [2] R. Ghez and S.S. Iyer, *The kinetics of fast steps on crystal surfaces and its application to molecular beam epitaxy of silicon*, IBM J. Res. Develop. **32** 804-818 (1988)
- [3] M.F. Gyure, C. Ratsch, B. Merriman, R.E. Caffisch, S. Osher, J.J. Zinck, D.D. Vvedensky, *Level-set methods for the simulation of epitaxial phenomena*, Phys. Rev. E **58** R6927 (1998).
- [4] S. Chen, B. Merriman, M. Kang, R.E. Caffisch, C. Ratsch, L.T. Cheng, M. Gyure, R.P. Fedkiw, C. Anderson S. Osher, *Level set method for thin film epitaxial growth*, J. of Comput. Phys. **167** 475 (2001).
- [5] C. Ratsch, M.F. Gyure, R.E. Caffisch, F. Gibou, M. Petersen M. Kang, J. Garcia, D.D. Vvedensky, *Level-set method for island dynamics in epitaxial growth*, Phys. Rev. B **65** 195403 (2002).
- [6] M. Petersen, C. Ratsch, R.E. Caffisch and A. Zangwill, *Level set approach to reversible epitaxial growth*, Phys. Rev. B **64** 061602 (2001).

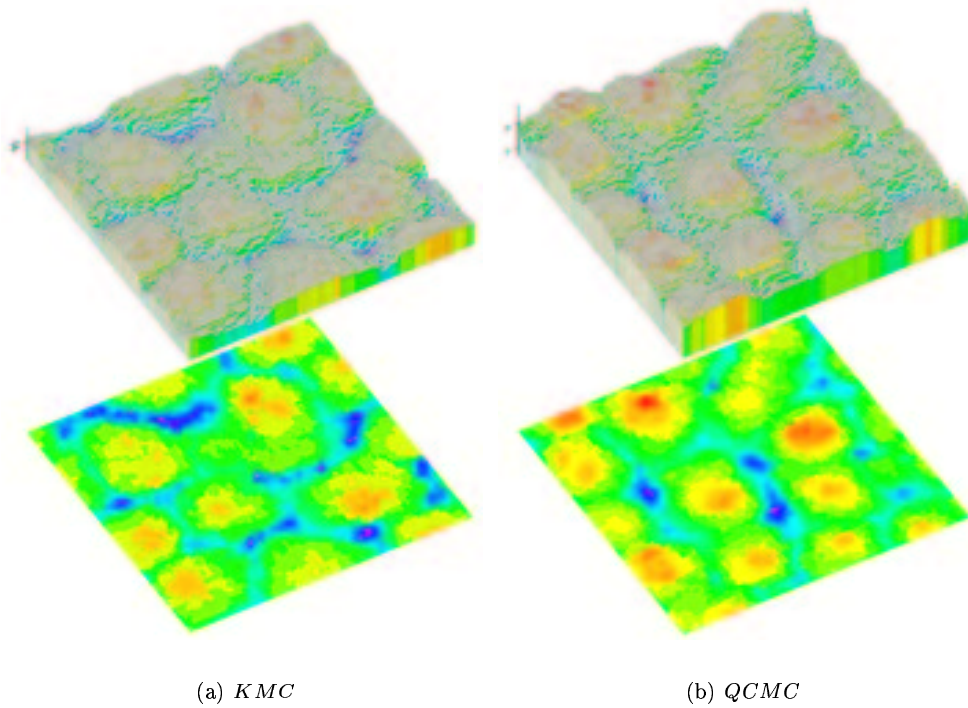


FIGURE 6. KMC versus QCMC for $E_s/kT = 1.26, E_0/kT = 3.5,$
 $F = 1.5 \times 10^{-4}, 90$ monolayers

- [7] J. Tersoff, M.D. Johnson, and B.G. Orr, *Adatom densities on GaAs: evidence for near-equilibrium growth*, Phys. Rev. Lett. **78** 282-285 (1997).
- [8] T.P. Schulze and W. E, *A continuum model for the growth of epitaxial films*, J. Cryst. Growth, **222** (2000) 414-425.
- [9] L. Mandreoli, J. Neugebauer, R. Kunert, and E. Schöll, *Adatom density kinetic Monte Carlo: A hybrid approach to perform epitaxial growth simulations*, Phys. Rev. B. **68**, 155429 (2003).
- [10] C. Ratsch, M. Kang and R.E. Caflisch, *Atomic size effects in continuum modeling*, Phys. Rev. E **64** 020601(R) (2001).
- [11] T.A. Witten and L.M. Sander, *Diffusion-Limited Aggregation, a Kinetic Critical Phenomenon*, Phys. Rev. Lett. **47**1400 (1981).
- [12] T.P. Schulze, P. Smereka, W. E, *Coupling kinetic Monte-Carlo and continuum models with application to epitaxial growth*, J. Comput. Phys. **189** (2003) 197-211.
- [13] T.P. Schulze, *A hybrid method for simulating epitaxial growth*, J. Cryst. Growth, to appear.

- [14] G. Russo, L.M. Sander, P. Smereka, *Quasicontinuum Monte Carlo: A method for surface growth simulations*, Phys. Rev. B **69** 121406(R) (2004).
- [15] G. Ehrlich, F. Hudda, *Atomic view of surface self-diffusion: tungsten on tungsten*, J. Chem. Phys. **44** 1039 (1966). R.L. Schwoebel, *Step motion on crystal surfaces II*, J. Appl. Phys. **40** 614 (1969).
- [16] L. Niemeyer, L. Pietronero, H.J. Wiesmann, *Fractal Dimension of Dielectric Break-down* Phys. Rev. Lett. **52** 1033 (1984).
- [17] J.A. Venables, *Rate equation approaches to thin film nucleation kinetics.*, Phil. Mag. **27** 697 (1973).
- [18] C. Rottman, M. Wortis, *Exact equilibrium crystal shapes at nonzero temperature in two dimensions*, Phys. Rev. B **24** 6274 (1981).
- [19] G.S. Bales, D.C. Chrzan, *Dynamics of irreversible island growth during submonolayer epitaxy*, Phys. Rev. B **50** 6057 (1984).
- [20] M.D. Johnson, C. Orme, A.W. Hunt, D. Graff, J. Sudijono, L.M. Sander, B.G. Orr, *Stable and unstable growth in molecular beam epitaxy*, Phys. Rev. Lett. **72** 116 (1994).
- [21] J.G. Amar and F. Family, *Mound Formation, Coarsening and Instabilities in Epitaxial Growth*, Surface Rev. and Lett. **5** 851-864 (1998).

Acknowledgment

This work is supported by the National Science Foundation. JPD and PS were supported by NSF grant number DMS 0207402. LMS and PS were supported by NSF grant number DMS 0244419.

Jason P. DeVita
Department of Physics
University of Michigan
Ann Arbor, MI, 48109-1120, USA
e-mail: jdevita@umich.edu

Leonard M. Sander
Department of Physics
and Michigan Center for Theoretical Physics
University of Michigan
Ann Arbor, MI, 48109-1120, USA
e-mail: lsander@umich.edu

Peter Smereka
Department of Mathematics
and Michigan Center of Theoretical Physics
University of Michigan
Ann Arbor, MI 48109-1109, USA
e-mail: psmerek@umich.edu